C-terminal phosphorylation of SPAK and OSR1 kinases promotes their binding and activation by the scaffolding protein MO25

by Binar Asring Dhiani

Submission date: 11-Aug-2022 08:31AM (UTC+0700)
Submission ID: 1881181190
File name: their_binding_and_activation_by_the_scaffolding_protein_MO25.pdf (1.38M)
Word count: 4748
Character count: 25326

Biochemical and Biophysical Research Communications 503 (2018) 1868–1873

Contents lists available at ScienceDirect

Biochemical and Biophysical Research Communications

journal homepage: www.elsevier.com/locate/ybbrc

C-terminal phosphorylation of SPAK and OSR1 kinases promotes their binding and activation by the scaffolding protein MO25

Youcef Mehellou [a, *], Mubarak A. Alamri [b], Binar A. Dhiani [a], Hachemi Kadri [a]

[a] School of Pharmacy and Pharmaceutical Sciences, Cardiff University, King Edward VII Avenue, Cardiff CF10 3NB, UK
[b] School of Pharmacy, College of Medical and Dental Sciences, University of Birmingham, Edgbaston, Birmingham B15 2TT, UK

ARTICLE INFO

Article history:
Received 9 July 2018
Accepted 24 July 2018
Available online 27 July 2018

Keywords:
SPAK
OSR1
Kinase
MO25
Phosphorylation

ABSTRACT

SPAK and OSR1 are two protein kinases that play important roles in regulating the function of numerous ion co-transporters. They are activated by two distinct mechanisms that involve initial phosphorylation at their T-loops by WNK kinases and subsequent binding to a scaffolding protein termed MO25. To understand this latter SPAK and OSR1 regulation mechanism, we herein show that MO25 binding to these two kinases is enhanced by serine phosphorylation in their highly conserved WEWS motif, which is located in their *C*-terminal domains. Furthermore, we show that this *C*-terminal phosphorylation is carried out by WNK kinases *in vitro* and involves WNK kinases in cells. Mutagenesis studies revealed key MO25 residues that are important for MO25 binding and activation of SPAK and OSR1 kinases. Collectively, this study provides new insights into the MO25-mediated activation of SPAK and OSR1 kinases, which are emerging as important players in regulating ion homeostasis.

1. Introduction

Ste20-related proline-alanine-rich kinase (SPAK) and oxidative-stress-responsive kinase 1 (OSR1) are two serine/threonine protein kinases that are involved in the regulation of cellular ion homeostasis [1,2]. The amino acid sequences of SPAK and OSR1 are 68% identical and share a highly conserved 92-amino acids *C*-terminal (CCT) domain that mediates their binding to upstream and downstream protein partners [3] (Fig. 1A). The involvement of SPAK and OSR1 kinases in regulating ion homeostasis is a result of their ability to manipulate the function of a series of sodium, potassium and chloride ion co-transporters, such as NKCC1 and 2, NCC and KCC [1,2] (Fig. 1A), which regulate blood pressure [4]. The activation of SPAK and OSR1 kinases is triggered by phosphorylation at their T-loops, T-185 for OSR1 and T233 for SPAK (Fig. 1A), by the WNK family of protein kinases [5] whose mutations cause hypertension in humans [6]. Beyond T-loop phosphorylation, WNK kinases are known to phosphorylate SPAK and OSR1 at serine residues on their *C*-terminal motif (www.phosphosite.org) though the roles of such phosphorylation remains unclear. The catalytic activity of WNK-phosphorylated SPAK and OSR1 kinases is further enhanced by binding to a scaffolding protein known as mouse protein 25 (MO25) [7]. In humans, two isoforms (α- and β-) of MO25, which share 79% sequence identity, exist and they form key components of numerous protein complexes that perform diverse biological functions [8]. The binding of MO25 to WNK-phosphorylated SPAK and OSR1 kinases leads to 80- to 100-fold increase in their *in vitro* catalytic activity, respectively [7]. In cells, siRNA knock-down of MO25α resulted in a significant reduction in SPAK and OSR1 phosphorylation of their physiological substrate NKCC1 [7].

Beyond binding to SPAK and OSR1 kinases, MO25α along with the pseudokinase STRADα forms a heterotrimeric complex with the tumor suppressor kinase LKB1 [9] that phosphorylates numerous AMPK-related kinases [10,11]. The crystal structure of this heterotrimeric protein complex [12] as well as that of MO25α in complex with STRADα [13] shows that one of the key regions of STRADα that is responsible for binding to MO25 is a *C*-terminal region that contains a WEF motif. Indeed, mutations in the WEF motif of STRADα resulted in a loss of binding to MO25α [12]. Sequence alignment of human SPAK and OSR1 kinases with human STRADα shows the WEF motif of STRADα (aa. 329–431) aligns perfectly with a conserved WEW motif on SPAK and OSR1 kinases, aa. 384–386 and 336–338, respectively (Supplementary Fig. S1) [7]. We previously showed that the WEW motif of SPAK and OSR1 was essential in binding MO25 as mutations in either tryptophan (W) residues in this motif resulted in a significant loss

* Corresponding author.
E-mail address: MehellouY1@cardiff.ac.uk (Y. Mehellou).

https://doi.org/10.1016/j.bbrc.2018.07.128
0006-291X/

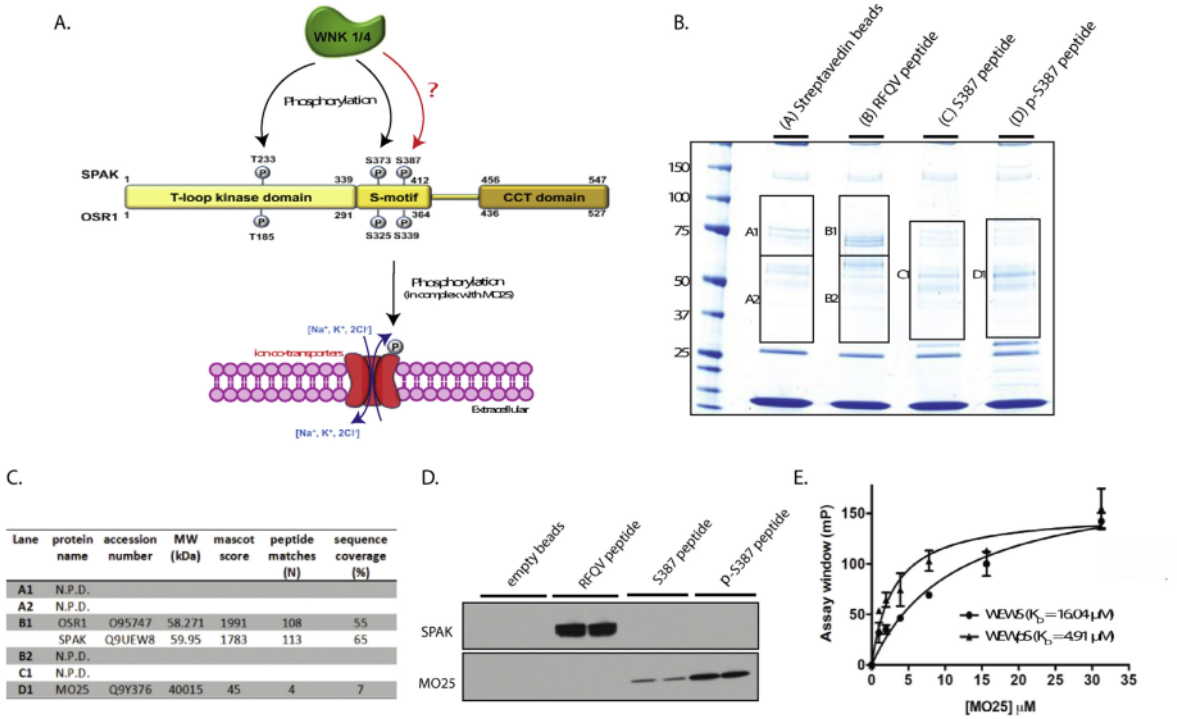

Lane	protein name	accession number	MW (kDa)	mascot score	peptide matches (N)	sequence coverage (%)
A1	N.P.D.					
A2	N.P.D.					
B1	OSR1	Q95747	58.271	1991	108	55
	SPAK	Q9UEW8	59.95	1783	113	65
B2	N.P.D.					
C1	N.P.D.					
D1	MO25	Q9Y376	40015	45	4	7

Fig. 1. Identification of proteins that bind OSR1 pS339. A. A general representation of the WNK-signalling cascade. WNK kinases phosphorylate SPAK and OSR1 at many residues on their T-loop and S-motif. Two phosphorylation sites are most prominent; OSR1 T185 and S325 and SPAK T233 and S373. SPAK and OSR1 phosphorylation at residues S387 and S339, respectively, is poorly understood. WNK-phosphoarylated SPAK and OSR1 kinases in complex with the scaffolding protein MO25 phosphorylate a series of sodium, potassium and chloride co-transporters. **B**. Coomassie stained gel of material pulled down from HEK293 cells using the *N*-terminally biotinylated 16-mer phosphopeptide C_{12}-TEDGDWEW**pS**DDEMDEK or its corresponding non phosphorylated peptide C_{12}-TEDGDWEW**S**DDEMDEK. These peptides correspond to amino acid residues 379–394 of human SPAK. The *N*-terminally biotinylated 18-mer peptide C_{12}-SEEGKPQLVGRFQVTSSK (RFQV peptide) derived from WNK1 (aa. 1006–1023) and empty streptavidin beads were used as controls. The bands that were excised and analysed by mass spec are shown in boxes. **C**. Summary of mass spectrometry results of the proteins identified from every band excised and shown in B. **D**. Confirmation of mass spectrometry results by western blotting. The biotinylated peptides used in the mass spectrometry pulldown experiment were incubated with HEK293 lysates. This was followed by streptavidin-biotin pulldown and western blotting for endogenous MO25 and SPAK. **E**. Fluorescence polarisation (FP) assay of MO25α binding to the phosphorylated and non-phosphorylated 16-mer WEW peptides. These peptides contained a CCPGCC *N*-terminal tag, which was used in the labelling with Lumio Green™. The fluorescence polarisation was measured using a PheraSTAR (excitation/emission) after the incubation of 10 nM of these peptides with recombinant MO25α at the indicated concentrations. The assay was run in triplicates. $n = 3$. (For interpretation of the references to colour in this figure legend, the reader is referred to the Web version of this article.)

of binding to MO25 that was translated into poor activation of SPAK and OSR1 [7]. The WEW motif of SPAK and OSR1 kinases is followed immediately by a serine residue while for STRADα such residue was not present as the WEF was the final motif of the protein sequence. Given that this serine residue is reported to get phosphorylated (www.phosphosite.org), we were intrigued by the possible impact of this phosphorylation on MO25 binding to SPAK and OSR1.

2. Material and methods

2.1. Reagents and standard experimental procedures

Detailed reagents and general experimental procedures such as immunoblotting and *in vitro* kinase assays are provided in the Supplementary Data.

2.2. Peptide pull-down and MS analysis

Cell lysates from HEK293 cells were centrifuged for 15 min at 14,000 rpm at 4 °C and the protein concentration was determined by Bradford. 15 mg of total protein lysate was precleared incubated 3 times with 15 μL of streptavidin beads. 3 mg of the precleared lysate was incubated with 3 μg of each of the following peptides: biotin-C_{12}-TEDGDWEWSDDEMDEK, biotin-C_{12}-TEDGDWEWS*D-DEMDEK or biotin-C_6- SEEGKPQLVGRFQVTSSK for 10 min at 4 °C under gentle agitation. This was followed by the addition of 15 μL of Streptavidin-Sepharose (pre-equilibrated in lysis buffer) slurry beads to every sample. As a reference, 3 mg of the precleared lysate was also incubated with 15 μL of Streptavidin-Sepharose (pre-equilibrated in lysis buffer) slurry beads. After further 5 min incubation at 4 °C under gentle agitation, the sample was centrifuged for at 5000 rpm at 4 °C for 2 min. The beads were subsequently washed twice with lysis buffer and twice with buffer A. The beads were then suspended in 40 μL of 1× SDS sample buffer, subjected to electrophoresis on a precast 4–12% gradient gel (Invitrogen) and the protein bands were visualized following Colloidal Blue staining. Proteins in the selected gel bands were reduced and alkylated by the addition of 10 mM DTT, followed by 50 mM iodoacetamide. Identification of proteins was performed by in-gel digestion of the proteins with 5 μg/mL trypsin and subsequent analysis of the tryptic peptides by LC (liquid chromatography)–MS/MS (tandem MS) on a Thermo LTQ-Orbitrap system coupled to a Thermo Easy nano-LC instrument. Excalibur RAW files were converted into peak

lists by Raw2msm [14] and then analysed by Mascot (http://www.matrixscience.com), utilizing the SwissProt human database. Two missed cleavages were permitted, the significance threshold was $P < 0.05$.

2.3. Fluorescence polarisation (FP) assay

The peptides used for the fluorescence polarisation (FP) assay were CCPGCCGGTEDGDWEWSDDEMDEK and CCPGCCGGTEDGDWEWpSDDEMDEK. The peptides were labelled with Lumio Green (Invitrogen) following the manufacturer's protocol. Fluorescence polarisation measurements were performed at room temperature in buffer containing 50 mM TrisHCl (pH 7.5), 200 mM NaCl and 5 mM DTT. Binding assays were performed by combining 10 nM labelled peptide with increasing concentrations of MO25α, in a total volume of 60 μL of buffer, and end-point polarisation measurements were made using the BMG PheraStar plate reader. The polarisation values were measured at an excitation wavelength of 485 nm and an emission wavelength of 538 nm, and were corrected for fluorescent probe alone. All data points were measured in triplicates. The data was analysed using GraphPad Prism 5 and curve-fitting of the data from two independent experiments was performed with one-site specific binding with Hill slope [model $Y = B_{max}X^h/(K_d^h + X^h)$] to determine K_d values as reported [15].

2.4. Pulldown and peptide competition assay

Wild-type (WT) Myc-tagged MO25α or the indicated mutants were overexpressed in HEK293 cells. Cell lysates (3 mg) were treated with 3 μg of biotinylated peptides [either phosphorylated (Biotin-C_{12}-TEDGDWEWpSDDEMDEK) or non-phosphorylated (Biotin-C_{12}-TEDGDWEWSDDEMDEK)]. Following streptavidin-biotin pull down and washing twice with lysis buffer and twice with buffer A, the material underwent blotting for Myc.

2.5. In silico docking

Autodock Vina 1.1.2 [16] was used for docking of WEW tripeptide into the human MO25α crystal structure (PDB: 1UPK) [17]. Initially, Discovery Studio 4.5 program (Accelrys, San Diego, CA, USA) was used to prepare the pdb files of MO25 protein, WEF and WEW peptides. AutoDock Tool 1.5.6 program was used to convert pdb files into pdbqt format [18]. The Grid box was set to cover the binding site of WEF using the following coordination in the Configuration input file (size_x = 18 size_y = 14 size_z = 16 center_x = 59.026 center_y = −41.500 center_z = 4.568). The docking results were visualized and analysed using PyMOL Molecular Graphics System 1.3.

3. Results and discussion

3.1. Serine phosphorylation of SPAK and OSR1 in the WEWS motif increases MO25 binding

In order to examine the importance of the conserved serine residue in the WEWS motif of SPAK and OSR1, we synthesised two 16-mer biotinylated peptides (biotin-C_{12}-TEDGD**WEWS**DDEMDEK) corresponding to amino acid residues 379–394 of human SPAK where in one peptide the serine residue adjacent to the WEWS motif was phosphorylated while it was unphopshorylated in the second peptide. In addition, we also synthesised an 18-mer biotinylated peptide biotin-C_{12}-SEEGKPQLVG**RFQV**TSSK (RFQV peptide) derived from WNK1 (aa. 1006–1023), which we had previously shown that it binds to endogenous SPAK and OSR1 [3]. We subsequently incubated these peptides with HEK293 cell lysates, which endogenously express MO25. Upon streptavidin-biotin pull down, the isolated material from each sample was analysed by mass spec to identify the proteins that bound each peptide (Fig. 1A and B). The material pulled down by the 18-mer RFQV peptide led to the precipitation of endogenous SPAK and OSR1 as expected [3]. Interestingly, the mass spec data showed that the 16-mer WEW peptide derived from SPAK, which had the serine residue phosphorylated, pulled down endogenous MO25 while its unphopshorylated peptide counterpart did not (Fig. 1C and D). To investigate this finding further, we repeated the streptavidin-biotin pull down from HEK293 cell lysates using the three different peptides and performed western blotting using SPAK and MO25 antibodies. The data showed that the positive control (18-mer RFQV) pulled down endogenous SPAK, while none of the other two 18-mer WEW peptides did (Fig. 1D). Strikingly, the peptide derived from SPAK bearing the phosphorylated serine residue within the WEWS motif pulled down a significantly larger amount endogenous MO25 as compared to the unphopshorylated peptide counterpart (Fig. 1D).

In order to measure the effect of SPAK S387 phosphorylation on MO25 binding, we developed a fluorescence polarisation (FP) assay that measures the binding affinity of the peptide derived from SPAK with S387 phosphorylated and that in which the same serine residue was not phosphorylated. The data showed that the peptide derived from SPAK in which S387 was phosphorylated had a higher affinity ($K_D = 4.91$ μM) for MO25 than its unphopshorylated counterpart ($K_D = 16.04$ μM) (Fig. 1E). This ca. 4-fold difference in binding affinity correlates with the results from the pull-down assay (Fig. 1D). Collectively, this data indicates that phosphorylation of SPAK at S387 enhances binding to MO25.

3.2. SPAK is phosphorylated at S387 in vitro and is not an autophosphorylation site

After establishing the role of SPAK phosphorylation at S387 in binding to MO25, we next investigated the possibility of SPAK S387 phosphorylation being carried out by WNK kinases. It is well known that WNK kinases phosphorylate SPAK at S373 on its C-terminal domain [5], but there have been no reports on WNK kinases phosphorylating SPAK at S387. To address this, we initially performed an *in vitro* kinase assay using recombinant WNK1 (1–667) and SPAK WT followed by western blotting for SPAK S373 and S387. The data showed that SPAK was phosphorylated *in vitro* by WNK1 at T233 and S373 as reported previously (Fig. 2) [5]. Interestingly, the data also showed that WNK kinases phosphorylated SPAK at S387. In addition, the data presented in Fig. 2 shows WNK1 WT was able to phosphorylate the three sites on SPAK WT and SPAK kinase-dead (KD) as expected. However, no phosphorylation of any of the three residues was detected when WNK1 KD was incubated with SPAK WT confirming that none of these three phosphorylation sites, including the newly identified SPAK S387, are autophosphorylation sites.

3.3. SPAK S387 is phosphorylation is WNK-dependent in cells

In order to determine if SPAK was phosphorylated at residue S387 by WNK kinases in cells, we stimulated HEK293 cells, which express endogenously the WNK-SPAK/OSR1-MO25 signalling components, with hypotonic buffer or sorbitol for different periods of time. Both hypotonic buffer and sorbitol has been shown to activate WNK-SPAK/OSR1 signalling in cells [14]. Upon cell lysis, the lysates were subjected to western blotting for SPAK S-motif phosphorylation; S373 and S387. As shown in Fig. 3A, the data shows that the treatment of HEK293 cells with either sorbitol or hypotonic buffer resulted in the phosphorylation of SPAK at S373,

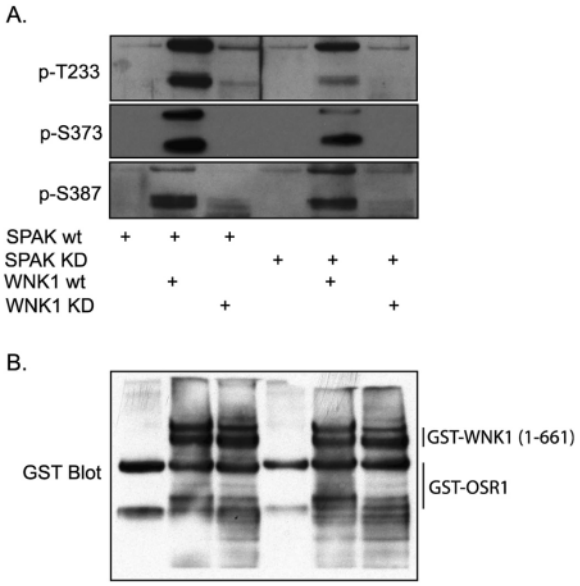

Fig. 2. Phosphorylation of SPAK at S387 *in vitro* by WNK kinases. A. *In vitro* kinase assay results showing phosphorylation of SPAK at S387 is not an autophosphorylation site. Recombinant human full length GST-tagged SPAK WT or KD were phosphorylated *in vitro* by recombinant human either GST-tagged WNK1 (1–699) WT or KD using 0.1 mM [γ-^{32}P]ATP and 10 mM $MgCl_2$ at 30 °C for 30 min. The material from each sample was then probed for SPAK T233, S373 and S387 phosphorylation by Western blotting. **B.** GST blot showing amounts of proteins (GST-SPAK WT and KD as well as GST WNK1 WT and KD) in each sample of the *in vitro* kinase assay.

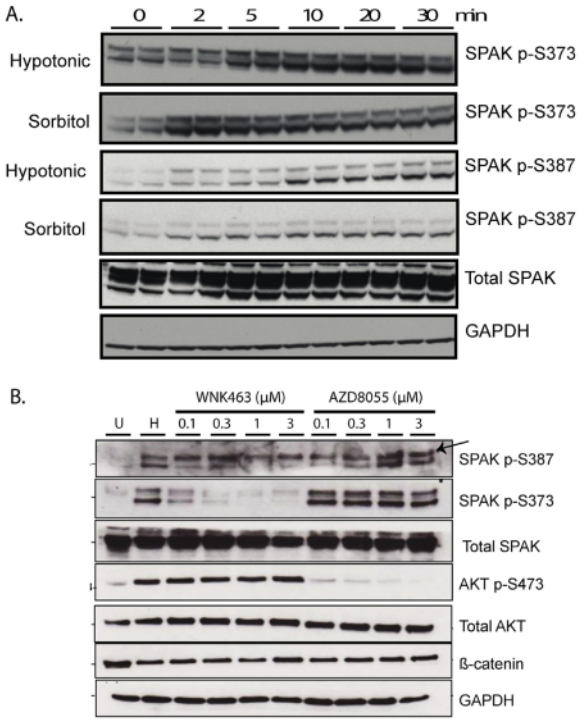

Fig. 3. SPAK phosphorylation at S387 is WNK1-dependent. A. HEK293 cells were stimulated with sorbitol or hypotonic low-chloride buffer for the indicated times. The cells were then lysed and subjected to immunoblot analysis with the indicated total and phospho-specific antibodies. * indicates a non-specific band. **B.** HEK293 cells were treated with low-chloride hypotonic buffer for 15 min. Then, they were treated with the WNK-signalling inhibitor WNK463 and the mTORC2 inhibitor AZD8055 at the indicated concentrations. Following cell lysis, the cell lysates were immunoblotted with the indicated total and phospho-specific antibodies. Similar results were obtained in three separate experiments.

as has been shown before [14]. Interestingly, the data also shows that SPAK was also phosphorylated at S387 following HEK293 cells stimulation by hypotonic buffer or sorbitol. This suggests that SPAK S387 phosphorylation is likely to be carried out in a WNK-dependent manner. Notably, OSR1 S339, which falls immediately after the WEW motif and aligns with SPAK S387, was reported to be directly phosphorylated by mTORC2 though the function of this phosphorylation site was not extensively studied [19]. To investigate whether the hypotonic buffer mediated phosphorylation of SPAK S387 that we observed in Fig. 3A is WNK- or mTORC2 phosphorylation, we repeated the experiment using the specific WNK inhibitor, WNK463 [20], and the mTORC2 inhibitor AZD8055 [21]. Confluent HEK293 cells were firstly treated with hypotonic buffer to activate WNK-signalling and then treated with varying concentrations of WNK463 or AZD8055. The results showed that WNK463 inhibited SPAK S373 phosphorylation in a concentration dependent manner as expected while AZD8055 had no effect on such phosphorylation (Fig. 3B). Also, AZD8055 inhibited mTORC2 phosphorylation of AKT at S473 whereas WNK463 had no effect on AKT phosphorylation by mTORC2 (Fig. 3B). Interestingly, cell treatment with WNK463 also led to a dose-dependent reduction of SPAK S387 phosphorylation while the mTORC2 inhibitor AZD8055 did not supress SPAK S387 phosphorylation (Fig. 3B). This indicated that SPAK S387 phosphorylation is likely to be WNK-dependent.

3.4. Mapping the interaction between SPAK/OSR1 and MO25

In order to understand where the conserved WEWS motif of SPAK and OSR1 binds to MO25, we performed *in silico* docking studies of the WEW motif into the crystal structure of MO25α (PDB: 1UPK). The docking revealed the WEW motif from SPAK/OSR1 docked in the same pocket on MO25α where the WEF of the pseudokinase STRADα was found to bind (Fig. 4A-C) [17]. This pocket had four key amino acid residues (K257, R264, K297 and K301), which appear to form interactions with the WEW motif (Fig. 4A–C). Notably, these same amino acids were verified previously as being important in binding STRADα [17]. To verify the obtained docking poses and the importance of these four amino acids, we mutated these MO25α residues and studied their effect on the MO25-dependent activation of SPAK and OSR1 kinases. Indeed, Myc-tagged MO25α mutants K257 M, K257F, R264A, K297 M and K301 M were cloned, expressed in *E. coli* (Supplementary Fig. S2) and studied their effect on the activation of SPAK T233E and OSR1 T185E *in vitro* using kinase assays as previously reported [7,22]. We used SPAK T233E and OSR1 T185E instead of SPAK WT and OSR1 WT as the glutamic acids mutants are introduced to mimic phosphorylation of these residues by WNK kinases [5]. The data shown in Fig. 4D and E reveals that mutating K301 to methionine (M) has the strongest effect on reducing the MO25-dependent activation of SPAK and OSR1. This was followed by mutating K257 to phenylalanine (F) while mutating this residue to a less bulkier amino acid, methionine (M) in this case, did not have as a significant effect as mutating it to methionine (M). Interestingly, mutations of R264 and K297 had little effect on the MO25-dependent activation of SPAK and OSR1 *in vitro*.

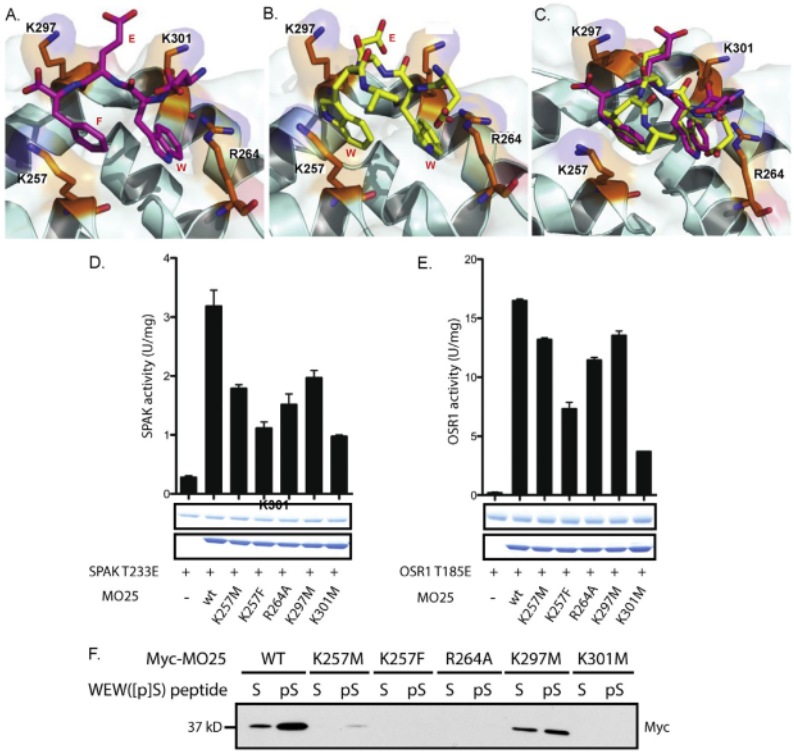

Fig. 4. Binding of SPAK and OSR1 the WEW tripeptide to MO25α. A. Figure showing the position of the key WEF motif (depicted in pink sticks) of STRADα in complex with human MO25α protein (PDB: 1UPK) as reported by Milburn et al. [17]. **B.** *In silico* docking of the conserved SPAK and OSR1 WEW motif i(depicted in yellow sticks) in the human MO25α protein (PDB: 1UPK). The key four amino acids [K257, R264, K297 and K301 (shown in brown sticks)] that fom a pocket in which the WEF/WEW motifs sit have been labelled. The WEF and WEW residues are labelled in red in A and B, respectively. **C.** Overlap of A and B with the key amino acids being labelled. WEF shown in pink sticks and WEW shown in yellow sticks. The part transparent MO25α protein surface shown. Details of the *in silico* docking are given under Materials and Methods. **D** and **E.** Effect of MO25α mutations on the *in vitro* activation of SPAK T233E and OST1 T185E respectively. Recombinant full-length human SPAK T233E and OSR1T185E 1–527 were purified from E. coli and used (0.22 μM) with the relevant MO25α WT or mutants (1 μM) to phosphorylate the peptide substrate CATCHtide *in vitro* for 30 min at 30 °C. 0.1 mM [γ-^{32}P]-ATP and 10 mM $MgCl_2$. The samples were run in triplicates. **F.** Myc-MO25 WT or the indicated mutants were overexpressed in HEK293 cells. Cell lysates (3 mg) were treated with biotinylated peptides (3 μg) either phosphorylated (Biotin-C_{12}-TEDGDWEWpSDDEMDEK) or non-phosphorylated (Biotin-C_{12}-TEDGDWEWSDDEMDEK). Following streptavidin-biotin pull-down the material underwent blotting for Myc. (For interpretation of the references to colour in this figure legend, the reader is referred to the Web version of this article.)

To explore the binding of these MO25α mutations to the phosphorylated and unphosphorylated SPAK/OSR1 WEWS motif, we overexpressed the MO25α Myc-tagged mutants (K257 M, K257F, R264A, K297 M and K301 M) in HEK293 cells (Supplementary Fig. S3). 200 μg from each cell lysate was incubated with 3 μg of either biotin-C_{12}-TEDGD**WEWS**DDEMDEK or biotin-C_{12}-TEDGD-**WEWpS**DDEMDEK. Following streptavidin-biotin, pull down the material underwent blotting for Myc. As shown in Fig. 4F, the phosphorylated WEWS peptide pulled down a more significant MO25α WT than its unphosphorylated counterpart. This is in agreement with the data shown in Fig. 1D. Interestingly, none of the other mutants were found to be pulled down by either the phosphorylated or unphosphorylated WEWS peptides. The only exception is the K297 M mutant, which seemed to bind the phosphorylated and unphosphorylated WEWS peptides in almost the same amount, though this was still significantly lower than the binding of the phosphorylated pep-tide to the MO25α WT. Together the data shows that K257 and K301 of MO25α play an important role in binding SPAK and OSR1 kinases.

In conclusion, we demonstrated that phosphorylation of SPAK and OSR1 in the serine residue adjacent to the WEW motif enhances binding to MO25. This serine phosphorylation is not an autophosphorylation site and in cells it is carried out in WNK-dependent manner. Furthermore, mutagenesis studies indicated key MO25α residues that are important for mediating the binding to SPAK/OSR1 kinases and their activation. Collectively, this work identifies an important role for the serine residue of the WEWS motif in the regulation of the catalytic activity of SPAK and OSR1 kinases by the scaffolding protein MO25.

Conflicts of interest

The authors declare that they have no competing interests.

Transparency document

Transparency document related to this article can be found online at https://doi.org/10.1016/j.bbrc.2018.07.128.

Appendix A. Supplementary data

Supplementary data related to this article can be found at https://doi.org/10.1016/j.bbrc.2018.07.128.

References

[1] D.R. Alessi, J. Zhang, A. Khanna, T. Hochdorfer, Y. Shang, K.T. Kahle, The WNK-SPAK/OSR1 pathway: master regulator of cation-chloride cotransporters, Sci. Signal. 7 (2014) re3.

[2] J. Hadchouel, D.H. Ellison, G. Gamba, Regulation of renal electrolyte transport by WNK and SPAK-OSR1 kinases, Annu. Rev. Physiol. 78 (2016) 367–389.

[3] A.C. Vitari, J. Thastrup, F.H. Rafiqi, M. Deak, N.A. Morrice, H.K. Karlsson, D.R. Alessi, Functional interactions of the SPAK/OSR1 kinases with their upstream activator WNK1 and downstream substrate NKCC1, Biochem. J. 397 (2006) 223–231.

[4] M. Murthy, T. Kurz, K.M. O'Shaughnessy, WNK signalling pathways in blood pressure regulation, Cell. Mol. Life Sci. 74 (2017) 1261–1280.

[5] A.C. Vitari, M. Deak, N.A. Morrice, D.R. Alessi, The WNK1 and WNK4 protein kinases that are mutated in Gordon's hypertension syndrome phosphorylate and activate SPAK and OSR1 protein kinases, Biochem. J. 391 (2005) 17–24.

[6] F.H. Wilson, S. Disse-Nicodeme, K.A. Choate, K. Ishikawa, C. Nelson-Williams, I. Desitter, M. Gunel, D.V. Milford, G.W. Lipkin, J.M. Achard, M.P. Feely, B. Dussol, Y. Berland, R.J. Unwin, H. Mayan, D.B. Simon, Z. Farfel, X. Jeunemaitre, R.P. Lifton, Human hypertension caused by mutations in WNK kinases, Science 293 (2001) 1107–1112.

[7] B.M. Filippi, P. de los Heros, Y. Mehellou, I. Navratilova, R. Gourlay, M. Deak, L. Plater, R. Toth, E. Zeqiraj, D.R. Alessi, MO25 is a master regulator of SPAK/OSR1 and MST3/MST4/YSK1 protein kinases, EMBO J. 30 (2011) 1730–1741.

[8] J. Boudeau, A.F. Baas, M. Deak, N.A. Morrice, A. Kieloch, M. Schutkowski, A.R. Prescott, H.C. Clevers, D.R. Alessi, MO25alpha/beta interact with STRADalpha/beta enhancing their ability to bind, activate and localize LKB1 in the cytoplasm, EMBO J. 22 (2003) 5102–5114.

[9] J. Boudeau, J.W. Scott, N. Resta, M. Deak, A. Kieloch, D. Komander, D.G. Hardie, A.R. Prescott, D.M. van Aalten, D.R. Alessi, Analysis of the LKB1-STRAD-MO25 complex, J. Cell Sci. 117 (2004) 6365–6375.

[10] J.M. Lizcano, O. Goransson, R. Toth, M. Deak, N.A. Morrice, J. Boudeau, S.A. Hawley, L. Udd, T.P. Makela, D.G. Hardie, D.R. Alessi, LKB1 is a master kinase that activates 13 kinases of the AMPK subfamily, including MARK/PAR-1, EMBO J. 23 (2004) 833–843.

[11] S.A. Hawley, J. Boudeau, J.L. Reid, K.J. Mustard, L. Udd, T.P. Makela, D.R. Alessi, D.G. Hardie, Complexes between the LKB1 tumor suppressor, STRAD alpha/beta and MO25 alpha/beta are upstream kinases in the AMP-activated protein kinase cascade, J. Biol. 2 (2003) 28.

[12] E. Zeqiraj, B.M. Filippi, M. Deak, D.R. Alessi, D.M. van Aalten, Structure of the LKB1-STRAD-MO25 complex reveals an allosteric mechanism of kinase activation, Science 326 (2009) 1707–1711.

[13] E. Zeqiraj, B.M. Filippi, S. Goldie, I. Navratilova, J. Boudeau, M. Deak, D.R. Alessi, D.M. van Aalten, ATP and MO25alpha regulate the conformational state of the STRADalpha pseudokinase and activation of the LKB1 tumour suppressor, PLoS Biol. 7 (2009) e1000126.

[14] A. Zagorska, E. Pozo-Guisado, J. Boudeau, A.C. Vitari, F.H. Rafiqi, J. Thastrup, M. Deak, D.G. Campbell, N.A. Morrice, A.R. Prescott, D.R. Alessi, Regulation of activity and localization of the WNK1 protein kinase by hyperosmotic stress, J. Cell Biol. 176 (2007) 89–100.

[15] J. van der Wijst, M.G. Blanchard, H.I. Woodroof, T.J. Macartney, R. Gourlay, J.G. Hoenderop, R.J. Bindels, D.R. Alessi, Kinase and channel activity of TRPM6 are co-ordinated by a dimerization motif and pocket interaction, Biochem. J. 460 (2014) 165–175.

[16] O. Trott, A.J. Olson, AutoDock Vina: improving the speed and accuracy of docking with a new scoring function, efficient optimization, and multithreading, J. Comput. Chem. 31 (2010) 455–461.

[17] C.C. Milburn, J. Boudeau, M. Deak, D.R. Alessi, D.M. van Aalten, Crystal structure of MO25 alpha in complex with the C terminus of the pseudo kinase STE20-related adaptor, Nat. Struct. Mol. Biol. 11 (2004) 193–200.

[18] M.F. Sanner, Python: a programming language for software integration and development, J. Mol. Graph. Model. 17 (1999) 57–61.

[19] S. Sengupta, A. Lorente-Rodriguez, S. Earnest, S. Stippec, X. Guo, D.C. Trudgian, H. Mirzaei, M.H. Cobb, Regulation of OSR1 and the sodium, potassium, two chloride cotransporter by convergent signals, Proc. Natl. Acad. Sci. U.S.A. 110 (2013) 18826–18831.

[20] K. Yamada, H.M. Park, D.F. Rigel, et al., Small-molecule WNK inhibition regulates cardiovascular and renal function, Nat. Chem. Biol. 12 (2016) 896–898.

[21] C.M. Chresta, B.R. Davies, I. Hickson, et al., AZD8055 is a potent, selective, and orally bioavailable ATP-competitive mammalian target of rapamycin kinase inhibitor with in vitro and in vivo antitumor activity, Canc. Res. 70 (2010) 288–298.

[22] Y. Mehellou, D.R. Alessi, T.J. Macartney, M. Szklarz, S. Knapp, J.M. Elkins, Structural insights into the activation of MST3 by MO25, Biochem. Biophys. Res. Commun. 431 (2013) 604–609.

C-terminal phosphorylation of SPAK and OSR1 kinases promotes their binding and activation by the scaffolding protein MO25

ORIGINALITY REPORT

17%	12%	15%	5%
SIMILARITY INDEX	INTERNET SOURCES	PUBLICATIONS	STUDENT PAPERS

MATCH ALL SOURCES (ONLY SELECTED SOURCE PRINTED)

2%

★ Karen T. Elvers, Magdalena Lipka-Lloyd, Rebecca C. Trueman, Benjamin D. Bax, Youcef Mehellou. "Structures of the Human SPAK and OSR1 Conserved C-Terminal (CCT) Domains", Cold Spring Harbor Laboratory, 2021

Publication

Exclude quotes	On	Exclude matches	Off
Exclude bibliography	On		